Shell model description of nuclei far from stability

N. Michel, W. Nazarewicz, J. Okolowicz, M. Ploszajczak, J. Rotureau

Shell model description of nuclei far from stability

N. Michel[1,2], W. Nazarewicz[1–3], J. Okołowicz[4,5], M. Płoszajczak[4], and J. Rotureau[4]

[1] Department of Physics and Astronomy, The University of Tennessee Knoxville, Tennessee 37996, USA

[2] Physics Division, Oak Ridge National Laboratory, P.O. Box 2008 Oak Ridge, TN 37831, USA

[3] Institute of Theoretical Physics, Warsaw University, ul. Hoża 69 PL-00681 Warszawa, Poland

[4] Grand Accélérateur National d'Ions Lourds (GANIL), CEA/DSM – CNRS/IN2P3, BP 55027, F-14076 Caen Cedex 05, France

[5] Institute of Nuclear Physics, ul. Radzikowskiego 152, PL-31342 Kraków, Poland

We shall discuss most recent advances in the description of weakly bound and unbound nuclear states using either a real ensemble representing (quasi-) bound single-particle states and scattering states (Shell Model Embedded in the Continuum) or a complex Berggren ensemble representing bound single-particle states, single-particle resonances, and non-resonant continuum states (the so-called Gamow Shell Model).

PACS numbers: 21.60.Cs, 24.10.Eq, 25.40.Lw, 27.20.+n

1. Introduction

Low-energy nuclear science is undergoing a revival with a technological revolution in the radioactive nuclear beam experimentation. New facilities have been built or are under construction, and new ambitious future projects will shape the research in this field for decades to come. From a theoretical point of view, the major problem is to achieve a consistent picture of weakly bound and unbound nuclei, which requires a synergy between nuclear structure and nuclear reactions. This ambitious quest for a unified description is

necessary because the spectroscopic information of nuclei that are close to the drip lines is dramatically affected by open channels.

The rigorous treatment of both the many-body correlations and the continuum of positive-energy states and decay channels is a challenging problem. Weakly bound states or resonances cannot be described within the closed quantum system formalism. For bound states, there appears a virtual scattering into the continuum phase space involving intermediate scattering states. Continuum coupling of this kind affects also the effective nucleon-nucleon interaction. For unbound states, the continuum structure appears explicitly in the properties of those states. The consistent treatment of continuum in multi-configuration mixing calculations is the domain of the continuum shell model (CSM) [1].

The impact of the particle continuum was discussed already in the early days of the multiconfigurational shell model (SM). For instance, the Thomas-Ehrman shift [2], which is a salient effect of a coupling to the continuum depending on the position of the respective particle emission thresholds, was well known in those days. However, the success of the 'standard' SM description in terms of interacting nucleons, assumed to be perfectly isolated from an external environment of scattering states, delayed the progress in the CSM for many decades. Below we shall discuss two recent developments in this area.

2. Shell Model Embedded in the Continuum

The mathematical formulation of the problem of nuclear states embedded in the continuum of decay channels goes back to Feshbach [3], who introduced the two subspaces containing the discrete (Q subspace) and scattering (P subspace) states. A unified description of nuclear structure and nuclear reaction aspects is much more involved and became possible in realistic situations much later (see Ref. [1] and references quoted therein). The Shell Model Embedded in the Continuum (SMEC) [4] offers a unified description of energy spectra, including nucleon emission widths, as well as the reactions involving one nucleon in the continuum, such as the (in)elastic proton scattering, radiative capture processes, Coulomb dissociation, first-forbidden beta decay, etc. (see Ref. [1] for a review). The first attempt to extend SMEC for two nucleons in the continuum can be found in this volume [5]. The SMEC formalism, in conjunction with the Feshbach projection technique, yields a precise description of radial wave functions at large distances which is a must for the description of nuclear reactions. All the coupling matrix elements between different discrete states, different scattering states, as well as between discrete and scattering states, are calculated in SMEC using the realistic effective SM interaction. Below, we shall discuss

certain features of the coupling to the particle continuum on the example of binding energy systematics.

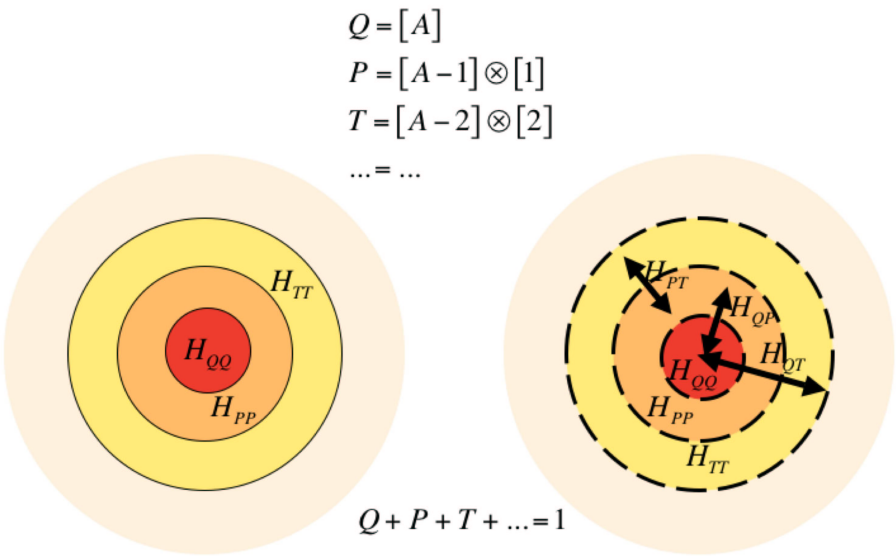

Fig. 1. Schematic representation of various Hilbert subspaces in SMEC: (i) uncoupled subspaces (left diagram) with different number of particles in the scattering continuum; (ii) coupled subspaces (right diagram).

The localized many-body states forming a Q-subspace are obtained by solving a standard SM problem for the Hamiltonian H_{QQ}. Asymptotic channels made of $(A-1)$-particle localized states and one nucleon in scattering states are contained in P-subspace. In T-subspace, two nucleons are in the scattering states and $(A-2)-$ occupy discrete orbits, and the division can go on (see Fig. 1). In the following, we shall discuss the case of coupled Q, P subspaces. The residual coupling (H_{PQ}) between these two subspaces is given by the zero-range interaction including the spin-exchange term [4]. An effective Hamiltonian in Q (see Fig. 2) including the coupling to the one-nucleon continuum is energy-dependent:

$$H_{QQ}^{(eff)}(E) = H_{QQ} + H_{QP}G_P^{(+)}(E)H_{PQ} \quad , \tag{1}$$

where $G_P^{(+)}(E)$ is the Green's function for the motion of a single nucleon in P. The second term on the r.h.s. of Eq. (1) generates effective three-body correlations in Q.

The energy scale is defined by the one-nucleon emission threshold $E^{(\mathrm{thr})}$ [4]. For $E > E^{(\mathrm{thr})}$, $H_{QQ}^{(eff)}$ is a complex-symmetric matrix, while for $E <$

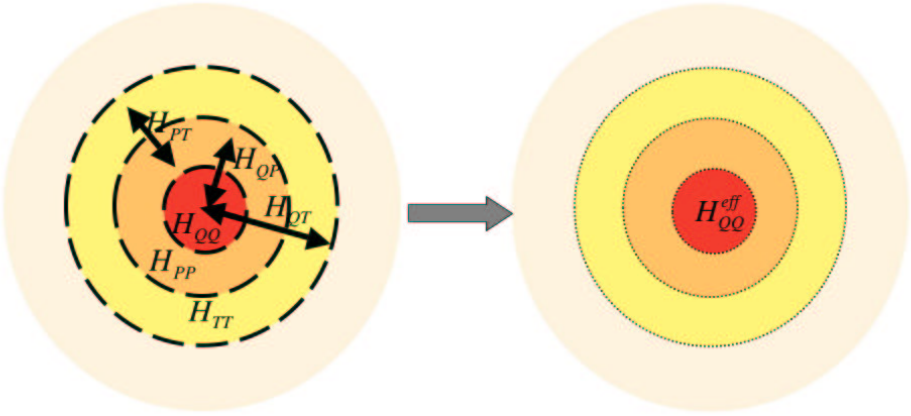

$$H_{QQ} \rightarrow H_{QQ}^{eff} = H_{QQ} + H_{QT}G_T^+(E)H_{TQ} + \\ +\left[H_{QP} + H_{QT}G_T^+(E)H_{TP}\right]\tilde{G}_P^+(E)\left[H_{PQ} + H_{PT}G_T^+(E)H_{TQ}\right]$$

$$\tilde{G}_P^+(E) = \left[E - H_{PP} - H_{PT}G_T^+(E)H_{TP}\right]^{-1}$$
$$G_T^+(E) = \left[E - H_{TT}\right]^{-1}$$

Fig. 2. Schematic representation of the transformation from coupled Hamiltonians in $Q + P + T$ to the effective Hamiltonian $H_{QQ}^{(eff)}$ in Q which contains the virtual coupling to remaining subspaces. $\tilde{G}_P^+$, G_T^+ are the Green's functions in P and T, respectively. (For more details see Ref. [5].)

$E^{(\mathrm{thr})}$ the matrix is hermitian, like in the ordinary SM. The ground state (g.s.) continuum coupling correction to the binding energy is given by [6]:

$$E_{\mathrm{corr}} = \langle \Phi_{\mathrm{g.s.}} | H_{QQ}^{(eff)} - H_{QQ} | \Phi_{\mathrm{g.s.}} \rangle \quad . \tag{2}$$

The g.s. wave function in the parent nucleus (N, Z) is coupled to different channel wave functions, which are determined by the motion of an unbound neutron relative to the daughter nucleus $(N-1, Z)$ in a certain SM state $\Phi_i^{(N-1)}$.

Figure 3 shows the neutron number dependence of E_{corr} in oxygen isotopes for (i) $E_n^{(\mathrm{thr})}$ of SMEC (solid line), and (ii) $E_n^{(\mathrm{thr})}$ fixed arbitrarily at 0 or 4 MeV. In the present study, we take the full *sd* valence space for $N < 20$ and the full *pf* space for $N > 20$. For H_{QQ}, we employ the USD interaction in the *sd* shell [7] and the KB$'$ interaction in the *pf* shell [8]. The cross-shell

interaction is given by the G-matrix of Ref. [9]. In our model space, the continuum coupling contains the neutron-neutron (T=1) part only.

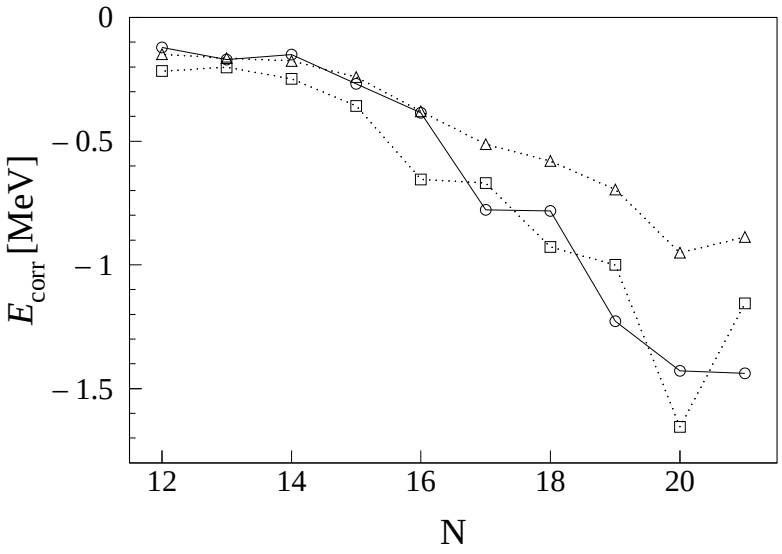

Fig. 3. Neutron number dependence of $E_{\rm corr}$ (2) to the SM g.s. energy for the neutron-rich oxygen isotopes. The solid line is obtained for the one-neutron emission threshold $E_n^{\rm (thr)}$ calculated in SMEC for each nucleus individually. The dotted lines with squares and triangles are obtained for $E_n^{\rm (thr)}$ fixed at 0 and 4 MeV, respectively.

A non-linear tendency in $E_{\rm corr}$ as a function of N (cf. Fig. 3) has two origins. Firstly, for a fixed value of $E_n^{\rm (thr)}$ (see the curve for $E_n^{\rm (thr)} = 4$ MeV), the continuum coupling induces an effective change $\delta V^{T=1}_{j_1 j_2} \sim (V^{(nn)})^2/V^{T=1}_{j_1 j_2}$ of the T=1 matrix elements of the two-body interaction $V^{T=1}_{j_1 j_2}$. This dependence, which is well seen in the matrix elements involving the $0d_{3/2}$ orbit, can be taken into account by a phenomenological adjustment of the T=1 two-body monopole terms of the effective two-body interaction. More important, however, is the change in an average behavior of $E_{\rm corr}$ due to the strong dependence on $E_n^{\rm (thr)}$. Close to the neutron drip line, this dependence leads to an effective enhancement of the strength of nn-continuum coupling which *cannot* be corrected by an N-independent correction of the two-body monopoles. A particle-number dependence of the two-body monopole terms may arise as a result of an approximation of the monopoles of the realistic interactions including a three-body force in the framework of the standard SM [10]. Here we demonstrate that the N-dependence arises naturally from the coupling between Q and P subspaces.

On top of the average behavior, one can see an odd-even staggering (OES) of $E_{\rm corr}(N)$. The OES near the one-neutron drip line (see the curve for $E_n^{\rm (thr)}=0$) is a characteristic feature of the T=1 continuum coupling. If $E_n^{\rm (thr)}$ is calculated in SMEC for each nucleus separately, the OES is inverted because $E_n^{\rm (thr)}$ in the odd-N nucleus is smaller than in even-N neighbors.

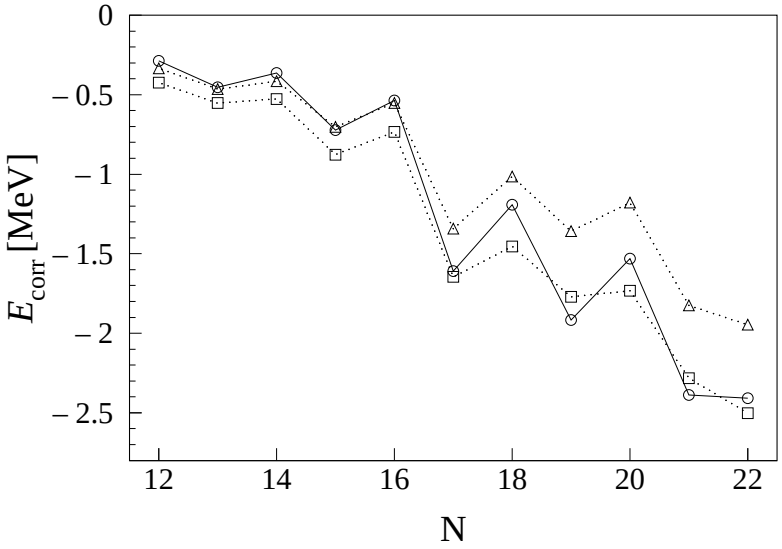

Fig. 4. Similar as in Fig. 3 except for the neutron-rich fluorine isotopes. The strength of the residual np-continuum coupling is $V_0^{(np)}=(1/2)V_0^{(nn)}$.

Figure 4 displays the neutron number dependence of $E_{\rm corr}$ for the fluorine isotopes. Here, both nn- (T=1) and np- (T=0,1) couplings between states in Q and P are active. The nn-coupling has been adjusted to the oxygen isotope chain. The np-contribution to $E_{\rm corr}$ dominates and, contrary to the nn-contribution, is independent of $E_n^{\rm (thr)}$. This implies that the change $\delta V_{j_1j_2}^{T=0}\sim (V^{(np)})^2/V_{j_1j_2}^{T=0}$ of the T=0 matrix elements induced by np-continuum coupling can be accounted for by a phenomenological adjustment of the T=0 monopole terms in the SM interaction. Different N-dependence of nn- and np-contributions to $E_{\rm corr}$ has, however, an important implication for the ratio $V_0^{(np)}/V_0^{(nn)}$, which gradually decreases when departing from the valley of stability towards the neutron drip line.

The three curves shown in Fig. 4 can be directly compared with those of Fig. 3. For $E_n^{\rm (thr)}=4$ MeV, one can see a strong OES which is absent in the oxygen chain. $E_{\rm corr}$ in odd-odd isotopes is increased as compared to odd-even neighbors. Qualitatively, a similar effect can also be seen at

the neutron drip line ($E_n^{(\mathrm{thr})} = 0$), but the np-coupling-induced OES is now attenuated by the nn-coupling. For the values of $E_n^{(\mathrm{thr})}$ calculated for each nucleus, the OES is enhanced due to the combined effects of the np-continuum coupling which weakly depends on $E_n^{(\mathrm{thr})}$, and the nn-continuum coupling which closely follows the OES of $E_n^{(\mathrm{thr})}$. These two effects act 'in phase', enhancing the binding of odd-N nuclei and strongly attenuating the OES indicator :

$$\Delta^{(3)}(N) = \frac{(-1)^N}{2}\left[E(N+1) - 2E(N) + E(N-1)\right] \tag{3}$$

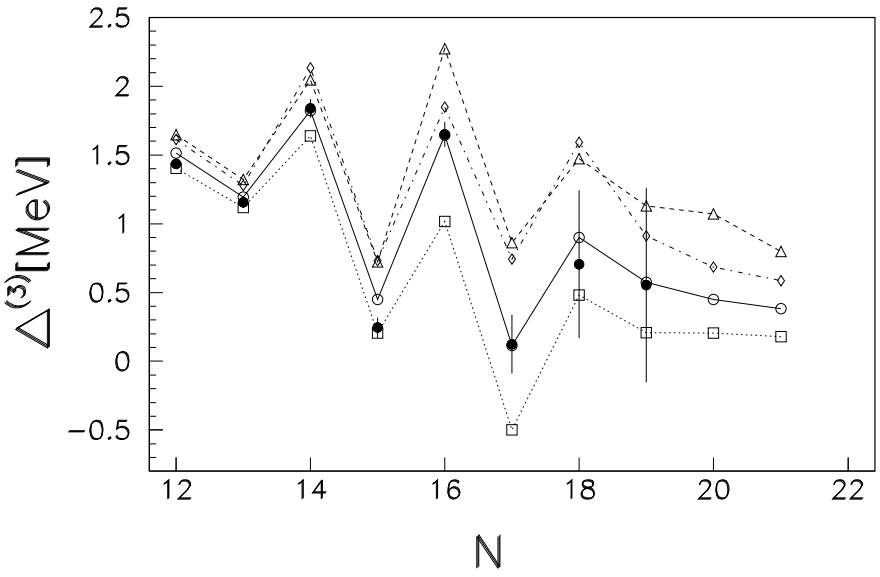

Fig. 5. The OES of binding energies (3) in fluorine isotopes calculated in SM (dashed line) and SMEC with different ratios of np- and nn-continum-coupling strengths: $V_0^{(np)} = (1/2)V_0^{(nn)}$ (solid line) and $V_0^{(np)} = 2V_0^{(nn)}$ (dotted line). The dashed-dotted line with open diamonds shows SM results for the USD+KB′ interaction without the modification of T=0,1 monopole terms. The filled dots with error bars show experimental data [11].

Interestingly, $\Delta^{(3)}(N)$ is very sensitive to the ratio $V_0^{(np)}/V_0^{(nn)}$. Figure 5 compares experimental values of $\Delta^{(3)}(N)$ in the fluorine isotopes with those calculated in SMEC and SM. It is seen that SM calculations systematically overestimate the OES effect, in particular in nuclei close to the neutron

drip line. On the contrary, the agreement of SMEC calculations assuming $V_0^{(np)} = (1/2)V_0^{(nn)}$ with experimental data is excellent for neutron-rich nuclei. A standard choice for nuclei close to the valley of stability, $V_0^{(np)} = 2V_0^{(nn)}$, is clearly excluded. Hence, the experimental data give an indication of the reduction in the ratio $V_0^{(np)}/V_0^{(nn)}$ in neutron-rich nuclei.

3. Gamow Shell-Model

Recently, the multiconfigurational continuum shell model in the complete Berggren basis, the so-called Gamow Shell Model (GSM), has been formulated [12, 13]. The single-particle (s.p.) basis of GSM is given by the Berggren ensemble [14] which contains Gamow (or resonant) states and the (complex) non-resonant continuum. The resonant states are the generalized eigenstates of the time-independent Schrödinger equation which are regular at the origin and satisfy purely outgoing boundary conditions. They correspond to the poles of the S-matrix in the complex energy plane lying on or below the positive real axis. One may see here a two-subspace concept of Feshbach reappearing, with the subspace Q_B consisting of resonant states in the complex energy plane, and the subspace P_B containing non-resonant scattering states.

GSM is a natural generalization of the SM concept in the complex k-plane for the description of open quantum systems: the number of particles in the scattering continuum is not predetermined, but it results from a variational calculation in the Hilbert space spanned by all Slater determinants in $Q_B + P_B$. As such, it can be even applied to 'super-Borromean' systems, such as the chain of helium isotopes $^{4-8}$He, for which A-, $(A-2)$- and $(A-4)$-nucleon systems are particle-stable but the intermediate $(A-1)$- and $(A-3)$-systems are not. One should stress that GSM is a tool *par excellence* for nuclear structure studies. The great advantage of GSM is its algorithmic simplicity and a similarity to the SM approach, which allows for fast progress in numerical techniques of solving the many-body problem in the continuum. Moreover, a formulation of the effective interaction theory in the Berggren basis will allow us in the future to understand the modification of the effective nucleon-nucleon interaction in weakly bound/unbound nuclear systems. On the other hand, a description of many-body wave functions at large distances, as needed in nuclear reaction studies, even though feasible within GSM formalism, may be rather cumbersome. For that purpose, the coupled-channel formalism used in SMEC to describe asymptotic channels is far more accurate.

3.1. Completeness relation involving Gamow states

There exist several completeness relations involving resonant states [15]. The cornerstone of GSM is the Berggren completeness relation [14] :

$$\sum_n |u_n\rangle\langle\tilde{u}_n| + \int_{L_+} |u_k\rangle\langle\tilde{u}_k| dk = 1 \quad , \tag{4}$$

where $|u_n\rangle$ are the Gamow states (both bound states and the decaying resonant states lying between the real k-axis and the complex contour L_+) and $|u_k\rangle$ are the scattering states on L_+. For neutrons, $l = 0$ resonances do not exist and, sometimes, one has to include the anti-bound $l = 0$ state in the Berggren completeness relation [16, 17]. This implies a modification of the complex contour L_+, which has to enclose this pole. In the neighborhood of a real-k axis, an $l = 0$ anti-bound state is strongly localized in the nuclear interior and plays an essential role in producing pairing correlations in weakly bound systems [18].

Resonant states are normalized according to the squared radial wave function and not to the modulus of the squared radial wave function. This is a consequence of the analytical continuation which is used to introduce the normalization of Gamow states. In practical applications, one has to discretize the integral in (4). Such a discretized Berggren relation is formally analogous to the standard completeness relation in a discrete basis of L^2-functions and, in the same way, leads to the eigenvalue problem $H|\Psi\rangle = E|\Psi\rangle$. However, as the formalism of Gamow states is non-hermitian, the matrix H is complex symmetric. The discretized Berggren basis can be a starting point for establishing the completeness relation in the many-body case in full analogy with the standard SM in a complete (discrete) basis of L^2-functions. One obtains :

$$\sum_n |\Psi_n\rangle\langle\tilde{\Psi}_n| \simeq 1 \quad , \tag{5}$$

where $|\Psi_n\rangle \equiv |\phi_1 \cdots \phi_N\rangle$ are the N-body Slater determinants, and $|\phi_m\rangle$ are the resonant (bound and decaying) and scattering (contour) s.p. states. The approximate equality in Eq. (5) is a consequence of the continuum discretization. As in the case of s.p. Gamow states, the normalization of Gamow-Slater determinants is given by the squares of SM amplitudes : $\sum_n c_n^2 = 1$ and not by the squares of their absolute values.

3.2. Determination of many-body bound and resonance states

In a standard SM, one often uses the Lanczos method to find the low-energy eigenstates (bound states) in very large configuration spaces. A

straightforward application of this method for the determination of many-body resonances is useless because of a continuum of surrounding many-body scattering states, many of them having lower energy than the resonances. A practical solution to this problem has been proposed in Ref. [12]:

- In the first step, one performs calculations in the pole approximation, *i.e.*, the Hamiltonian is diagonalized in a smaller basis consisting of s.p. resonant states only. Here, some variant of the Lanczos method can be applied. The diagonalization yields the first-order approximation to many-body resonances $|\Psi_i\rangle^{(0)}$, where index i ($i = 1, \ldots, N$) enumerates all eigenvectors in the restricted space. These eigenvectors serve as starting vectors (pivots) for the second step of the procedure.

- In the second step, one includes couplings to non-resonant continuum states in the Lanczos subspace generated by $|\Psi_j\rangle^{(0)}$ ($j \in [1, \ldots, N]$).

- Finally, one searches among the M solutions $|\Psi_{j;k}\rangle$, ($k = 1, \ldots, M$), for the eigenvector which has the largest overlap with $|\Psi_j\rangle^{(0)}$.

3.3. GSM Study of Helium Isotopes

A description of neutron-rich helium isotopes, including Borromean nuclei ^{6,8}He, is an exciting theoretical problem. The nucleus ^{4}He is a well-bound system with the one-neutron emission threshold at 20.58 MeV. On the contrary, the nucleus ^{5}He is a broad resonance. The nucleus ^{6}He, which consists of two neutrons outside ^{4}He, is bound with the two-neutron emission threshold at 1.87 MeV. Again, ^{7}He is a broad resonance (cf. Fig. 7) and ^{8}He is bound even stronger than ^{6}He.

In the GSM calculations, the s.p. configuration space includes both resonances $0p_{3/2}$, $0p_{1/2}$ and the two associated complex continua $p_{3/2}$ and $p_{1/2}$ which are discretized with 5 points each. At present, the main limitation of GSM is the explosion of the number of s.p. configuration space, as compared to the traditional SM. For each partial wave (l, j), one needs to include all the relevant Gamow states (bound, resonant or $l = 0$ anti-bound) as well as the corresponding discretized continua represented by a set of shells $[(l, j)^{(c_1)}, (l, j)^{(c_2)}, \cdots, (l, j)^{(c_n)}]$, where n is the number of points along the discretized contour. To deal with this problem in GSM, one may develop techniques borrowed from the Density Matrix Renormalization Group method [19]. Obviously, these techniques have to be generalized for the genuinely non-hermitian formalism of the GSM. The first attempts in this direction have been made recently by Rotureau et al. [20] in the j-scheme GSM.

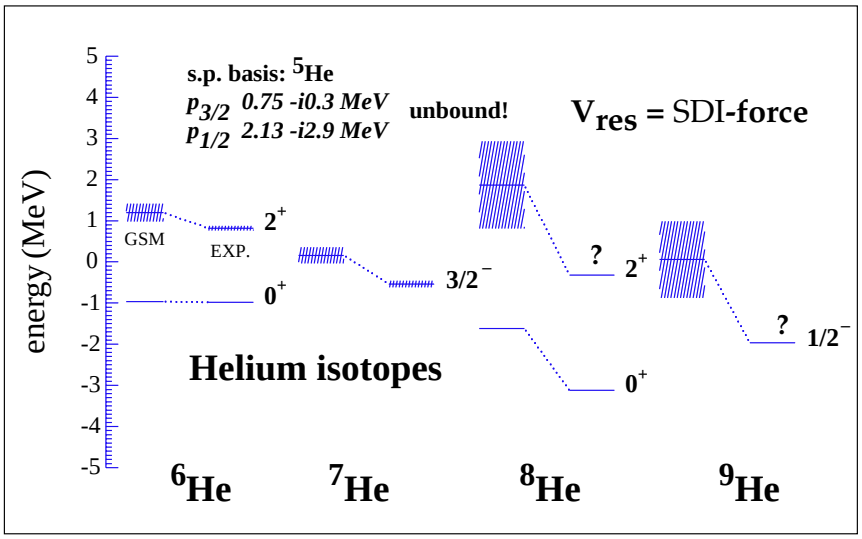

Fig. 6. Experimental (EXP) and calculated (GSM) binding energies of $^{6-9}$He as well as energies of $J^\pi = 2^+$ states in ^{6}He and ^{8}He. The resonance widths are indicated by shading. The energies are given with respect to the core of ^{4}He.

Figure 6 shows the lowest energy states of helium isotopes calculated with the surface delta interaction with the strength $V_{SDI} = 1670$ MeV·fm^3. The $0p_{3/2}$, $0p_{1/2}$ s.p. resonances are generated by a Woods-Saxon (WS) potential with the parameters chosen to reproduce experimental energies and widths of the $3/2^-_1$ and $1/2^-_1$ resonances of ^{5}He.

It is found that the non-resonant continuum contributions are *always essential* and, in some cases (e.g., ^{8,9}He), they dominate the structure of the g.s. wave function. Moreover, the wave function components having many neutrons in the non-resonant continuum give a large contribution to the binding energy. While without the non-resonant (contour) states, the predicted g.s. energy of ^{8}He is predicted to be $+2.08$ MeV; the inclusion of scattering states lowers the binding energy to -1.6 MeV. GSM calculations reproduce the most important feature of ^{6,8}He: *the ground state is particle bound despite the fact that all the basis states lie in the continuum.* The neutron separation energy anomaly, i.e., the *increase* of one-neutron separation energy when going from ^{6}He to ^{8}He, is reproduced. This anomaly is explained in GSM by a large contribution from non-resonant continuum states.

The odd-N isotopes of ^{5,7,9}He are calculated to be wide neutron res-

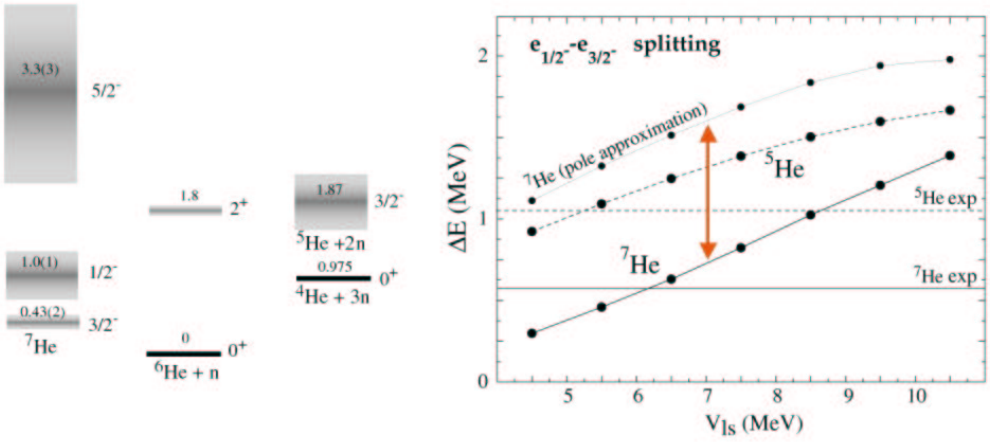

Fig. 7. Left: spectrum of ^{7}He (from Ref. [26]). Right: The energy splitting of $I^\pi = 3/2^-$ (ground state) and $I^\pi = 1/2^-$ (first-excited) resonance states in ^{5}He (dashed line) and ^{7}He (solid line) calculated for different strength V_{ls} of the WS potential. The dotted line for ^{7}He has been calculated in the pole approximation, neglecting the contribution from the (contour) non-resonant continuum states.

onances. In ^{5,7}He, both g.s. ($I^\pi = 3/2^-$) and first-excited ($I^\pi = 1/2^-$) resonance states have been studied experimentally. It is then interesting to compare the experimental splitting of $I^\pi = 3/2^-$ and $1/2^-$ resonances in ^{5,7}He with GSM results. Usually, the $I^\pi = 1/2^-$ state in ^{7}He was identified with the structure found at the excitation energy $E^* \sim 3$ MeV [21]. All previous theoretical studies, including quantum Monte Carlo calculations [22], conventional shell model [23, 24], or resonating group model calculations [25], predict at around this excitation energy the $1/2^-$ state and agree qualitatively with these data. Recently, however, Meister *et al.* [26] have reported in the relative energy spectrum in the ^{6}He + n system a new resonance ($I^\pi = 1/2^-$) at the excitation energy $E^* \sim 0.6$ MeV above the g.s. of ^{7}He, in striking disagreement with all earlier theoretical studies. This new data implies that the energy splitting of $3/2^-_1$ and $1/2^-_1$ resonances in ^{7}He is smaller than in ^{5}He. Fig. 7 compares this energy splitting calculated in GSM with the experimental data. The calculations are performed for different strengths V_{ls} of the spin-orbit term in the WS potential generating $3/2^-_1$ and $1/2^-_1$ s.p. resonances in ^{5}He. The strength of the surface delta

interaction is adjusted for each V_{ls} to reproduce the binding energy of ^{6}He relative to ^{4}He. With this input, the $I^\pi = 3/2^-_1$, $1/2^-_1$ energy splitting in ^{7}He is calculated in two ways : (i) in the pole approximation (the dotted line), *i.e.*, neglecting (contour) states of the non-resonant continuum, and (ii) in the full GSM (solid line). The energy splitting is strongly diminished by couplings to the non-resonant $(p_{3/2}, p_{1/2})$ continuum and the $I^\pi = 3/2^-_1$, $1/2^-_1$ splitting in ^{7}He is reduced. Currently, we are carrying calculations with finite-range residual interactions to check the robustness of this conclusion.

The few selected examples of CSM calculations presented in this work illustrate new phenomena in discrete/continuum spectroscopy of exotic nuclei. These phenomena appear due to the configuration mixing and couplings in the space of discrete (bound, anti-bound, decaying) and non-resonant continuum states. They also mark the emergence of a new paradigm of theoretical nuclear physics near drip lines: *the open quantum many-body system.*

This work was supported in part by the U.S. Department of Energy under Contract Nos. DE-FG02-96ER40963 (University of Tennessee) and DE-AC05-00OR22725 with UT-Battelle, LLC (Oak Ridge National Laboratory + KBN), and by the Polish Committee for Scientific Research (KBN) under Contract No. 5 P03B 014 21.

REFERENCES

[1] J. Okołowicz, M. Płoszajczak and I. Rotter, Phys. Rep. **374** (2003) 271.
[2] J.B. Ehrman, Phys. Rev. **81** (1951) 412; R.G. Thomas, Phys. Rev. **81** (1951) 148.
[3] H. Feshbach, Ann. Phys. (N.Y.) **5** (1958) 357 and **19** (1962) 287.
[4] K. Bennaceur, F. Nowacki, J. Okołowicz and M. Płoszajczak, Nucl. Phys. **A651** (1999) 289 and **A671** (2000) 203.
[5] J. Rotureau, J. Okołowicz and M. Płoszajczak, in this volume.
[6] Y. Luo, J. Okołowicz, M. Płoszajczak and N. Michel, nucl-th/0201073.
[7] B. H. Wildenthal, Prog. Part. Nucl. Phys. **11** (1984) 5.
[8] A. Poves and A. Zuker, Phys. Rep. **70** (1981) 4.
[9] S. Kahana, H. C. Lee and C. K. Scott, Phys. Rev. **180** (1969) 956 (1969).
[10] A. Zuker, Phys. Rev. Lett. **90** (2003) 042502.
[11] G. Audi and A. H. Wapstra, Nucl. Phys. **A595** (1995) 409.
[12] N. Michel, W. Nazarewicz, M. Płoszajczak and K. Bennaceur, Phys. Rev. Lett. **89** (2002) 042502.
[13] N. Michel, W. Nazarewicz, M. Płoszajczak and J. Okołowicz, Phys. Rev. **C67** (2003) 054311.
[14] T. Berggren, Nucl. Phys. **A109** (1968) 265.
[15] P. Lind, Phys. Rev. C **47**, 1903 (1993).

[16] R.Id. Betan, R.J. Liotta, N. Sandulsecu and T. Vertse, nucl-th/0307060; T. Vertse, private communication.
[17] G. Hagen, M. Hjorth-Jensen and J.S. Vaagen, nucl-th/0303039.
[18] K. Bennaceur, J. Dobaczewski and M. Płoszajczak, Phys. Rev. **C60** (1999) 034308.
[19] S.R. White, Phys. Rev. **B48** (1993) 10345.
[20] J. Rotureau, N. Michel, W. Nazarewicz, M. Płoszajczak and J. Dukelsky, to be published.
[21] A.A. Korsheninnikov et al., Phys. Rev. Lett. **82** (1999) 3581;
H.G. Bohlen et al., Phys. Rev. **C64** (2001) 024312;
M.G. Gornov et al., Bull. Rus. Acad. Sci. Phys. **62** (1998) 1781.
[22] R.B. Wiringa, Nucl. Phys. **A631** (1998) 70c;
R.B. Wiringa et al., Phys. Rev. **C62** (2000) 014001;
B.S. Pudliner et al., Phys. Rev. Lett. **74** (1995) 4396; Phys. Rev. **C56** (1997) 1720.
[23] N.A.F.M. Poppelier, A.A. Wolters and P.W.M. Glaudemans, Z. Phys. **A346** (1993) 11.
[24] P. Navratil and B.R. Barrett, Phys. Rev. **C57** (1998) 3119.
[25] J. Wurzer and H.M. Hofmann, Phys. Rev. **C55** (1997) 688.
[26] M. Meister et al., Phys. Rev. Lett. **88** (2002) 102501.